Optical Vortex Solitons Observed in Kerr Nonlinear Media

G. A. Swartzlander, Jr.,[1] and C. T. Law[2]

[1]*Laser Physics Branch, Code 6546, Naval Research Laboratory, Washington, D.C. 20375-5320*

[2]*Department of Electrical and Computer Engineering, The Johns Hopkins University, Baltimore, Maryland 21218*

(Received 5 March 1992; revised manuscript received 8 July 1992)

Optical vortex-soliton filaments are observed in a bulk self-defocusing Kerr nonlinear refractive medium. The dark cylindrical core, located at the axis of a 2π helical phase ramp, is stationary and stable, with a size that depends inversely on the field strength. Wave guiding of a weak probe beam within the core is reported. A single optical vortex soliton was experimentally created using a quasihelical phase mask. Pairs having opposite topological charge were experimentally and numerically investigated using a convective Kelvin-Helmholtz instability of dark soliton stripes.

PACS numbers: 42.50.Rh, 03.65.Ge, 42.65.Jx, 67.40.Vs

It is well known that an intense light beam induces refractive index changes in many materials. In a self-defocusing-type medium, the refractive index decreases with intensity, and owing to the law of refraction, the beam spreads into regions of low intensity. A Gaussian spatial intensity profile, for example, will induce a negative "lens" in the medium resulting in accelerated beam diffraction [1]. This "blooming" effect has limited uses. Richer nonlinear dynamics and opportunities to develop more elegant devices are possible by introducing a nonplanar phase profile in the transverse cross section of the field. Perhaps the most fundamental two-dimensional phase profile for a scalar wave is the vortex, i.e., an angular 2π phase ramp. In this Letter we report the first observations of optical vortices in a self-defocusing medium where the field propagates as a soliton, owing to the counterbalanced effects of diffraction and nonlinear refraction, which respectively broaden and narrow the interference trough (or core) at the phase singularity. This dark vortex core is stable and stationary [2], and appears as a dark filament within a bright background field. The optical vortex soliton (OVS) is the only known cylindrical soliton in nonlinear refractive media [3]. In contrast to vortices in linear media which are governed by the superposition principle [4] (i.e., they diffract), these nonlinear waves are stationary, and can be shown to obey hydrodynamic principles, as do nonlinear waves in other systems, such as slightly detuned laser cavities [5].

Under high intensities a Kerr nonlinearity is most frequently encountered (at least initially), i.e., $n=n_0+n_2|E|^2/2\equiv n_0-\Delta n$, where n_0 is the linear index, n_2 is a nonlinear coefficient, and E is the field amplitude profile in the transverse plane, (x,y) or (r,θ). The self-focusing case ($n_2>0$) is unstable and leads to catastrophic beam collapse [6,7]. Despite its inherent stability [8], the defocusing case ($n_2<0$) has attracted less interest. The (2+1)-dimensional nonlinear Schrödinger (NLS) equation describes propagation through a bulk defocusing medium:

$$[i\partial/\partial Z+\nabla_\perp^2-2|u|^2]u=0\,, \tag{1}$$

where $u=E/E_\infty$ is the normalized field amplitude, $|E_\infty|^2/2$ is the background intensity (i.e., at $R\rightarrow\infty$), and $R=r/w_{\rm NL}$ and $Z=z/z_{\rm NL}$ are the normalized radial and longitudinal coordinates, respectively, with $w_{\rm NL}^{-1}=k_0(\Delta n_{\rm NL}/n_0)^{1/2}$ and $z_{\rm NL}^{-1}=k_0\Delta n_{\rm NL}/2n_0$, k_0 the wave number, and $\Delta n_{\rm NL}=-n_2|E_\infty|^2/2$. The transverse Laplacian $\nabla_\perp^2$ accounts for diffraction, i.e., the creation of transverse wave vectors $\mathbf{k}_\perp$ which are redirected by the nonlinear term $2|u|^2$. The nonlinearity tends to make the beam more planar when $n_2<0$, i.e., the variance (or rms value) of $\mathbf{k}_\perp$ decreases with increasing intensity. This can be shown by calculating the expectation integral of the Fourier-transformed wave equation and writing $k^2=(k-\delta k_z)^2+(\delta k_\perp)^2$. We obtain $\mathrm{var}(\delta k_\perp)=\mathrm{var}(\delta k_\perp)_0-2k_0^2\langle\eta(k)/n_0\rangle$, where $\mathrm{var}(\delta k_\perp)_0$ is the linear variance of the transverse wave vector, and $\eta=\mathrm{FT}[\Delta nE]/\mathrm{FT}[E]$ is a ratio of Fourier transforms. This minimization of the variance may be interpreted as a global generalization of Fermat's principle applied to nonlinear optics, e.g., the system finds the state which minimizes the rms optical path length in a self-defocusing medium. (In contrast, the variance of the angular spectrum increases in a self-focusing system.) Qualitatively we find that for a highly nonlinear system, the beam structure collapses into narrow dark filaments having phase singularities. Turbulence and chaos may be expected when higher-order effects like dispersion are included.

The single-vortex solution of Eq. (1) is written [2]

$$u(R,\theta,Z)=A(R)\exp(iM\theta)\exp(i2Z)\,, \tag{2}$$

where $M=\pm1$ is topological charge, $A(0)=0$, $A(r\rightarrow\infty)\rightarrow1$, and our numerical calculations show that $A(R)\approx\tanh(R/R_0)$, where $R_0\approx1.270$ is a constant. (This amplitude function produces less than 0.5% fluctuations in the beam size, negligible radiation, and a correlation coefficient of 0.999 when compared to the numerical solution.) This stationary wave can be called a soliton because small-scale perturbations do not produce instabilities [8]. The field profile along a line through the vortex center is identical to that of a fundamental dark soliton stripe (DSS) [9,10] (up to the scale size R_0), with both having a π phase discontinuity. Whereas a DSS has rectilinear symmetry in the plane and the phase step defines

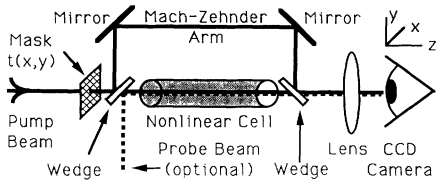

FIG. 1. Experimental apparatus. A laser beam passes through a mask with transmittance $t(x,y)$ near the input face of a nonlinear cell having $n_2 < 0$. The Mach-Zehnder interferometer allows phase measurements. A probe can be made to copropagate with the pump beam to observe wave guiding.

a domain wall, an OVS has circular symmetry. This is analogous to states in type-I and type-II superconductors. Because experiments require beams of finite size, the gross effects of diffraction and self-defocusing will reduce the field strength as the beam area widens. We numerically confirmed that $|E(z)|^2_{\text{peak}} w^2_{\text{NL}}(z) \approx (k_0^2 |n_2|)^{-1}$ remains relatively constant as long as the beam size is much larger than w_{NL}.

Because plane waves are stable in defocusing media, an initial field profile is required to initiate nonlinear waves. This is done experimentally by placing a thin mask with complex transmittance $t(x,y)$ near the input face of the nonlinear cell (see Fig. 1). The output face of the nonlinear cell is imaged on a charge-coupled-device (CCD) camera to record either the intensity profile, or an interferogram of the phase profile using a Mach-Zehnder interferometer. The experiments were performed in a cell of length 22 cm, containing slightly absorbing liquid [1], and using a collimated cw argon ion (514 nm) laser beam with diameter ≈ 2.5 mm. A single vortex can be formed using a helical phase mask $t = \exp(i\theta)$; however, to avoid the difficulty in forming such a mask, we used the simplest approximation: three regions with uniform phase retardations (0, π, and 2π), as shown in the inset of Fig. 2. The intensity profile [Fig. 2(a)] shows a black node, as expected, at the output face of the cell. This node is confirmed to be a vortex in the interferogram [Fig. 2(b)], which shows two equiphase lines converging into one (this vortex signature was observed at any angle of the reference wave). Our observations also confirmed that the node size was stable and could be decreased by increasing

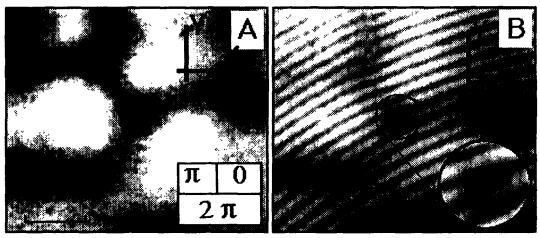

FIG. 2. Single-vortex-soliton experimental observations. (a) Intensity profile obtained with the phase mask shown in the inset. (b) Interferogram of (a), with magnified view of vortex region shown. The scale is 250 μm.

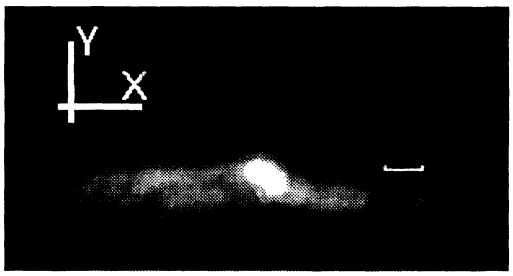

FIG. 3. Wave guiding of a He-Ne probe laser beam within an OVS filament. The phase mask in Fig. 2 was used, resulting in some leakage to dark soliton stripes. A wire of width 250 μm shows the relative size of the filament.

the field intensity. Owing to the higher relative index with the OVS, we were able to observe wave guiding of a (He-Ne laser) probe beam within the filament. The intensity profile of the guided beam (with the pump beam filtered out) is shown in Fig. 3. The bright arms extending from the filament are an artifact of the three-region mask, which also produces DSS's that can guide light. Such leakage may be avoided by using a helical phase mask. This vortex waveguiding technique could be used as an ultrafast high-gain modulator, controlled by a temporally modulated pump beam. Radiation pressure within the core allows other applications.

We now explain how OVS's can form even when vortices are not initially present (for example, when the phase profile is initially flat, rather than helical). To conserve the net topological charge $\sum_i M_i$ in this case, we expect vortices to appear as oppositely charged pairs. Our numerical solutions of Eq. (1) reveal that many initial diffraction conditions can spawn such OVS pairs. To describe how vorticity can develop in these cases, we consid-

Figure 4

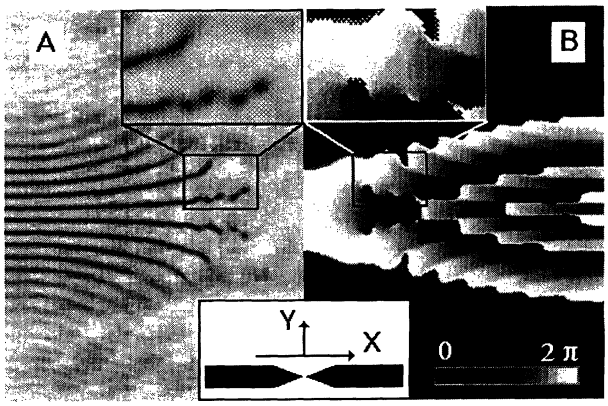

FIG. 4. Numerical calculations of intensity (a) and phase (b) profiles for nonlinear propagation past two needles, as shown in the bottom inset. Outside of the shadow region the solitons decay gracefully into the background. When subjected to long-period transverse perturbations, vortex pairs of opposite topological charge are formed owing to a Kelvin-Helmholtz instability.

er a simple amplitude mask that displays all the essential physical processes. The inset in Fig. 4 shows the initial condition, which in practice can be formed by aligning two needles along the x axis with tips facing each other. Because the mask is nearly rectilinear, both one- and two-dimensional nonlinear phenomena, i.e., soliton stripes and vortices, may be expected. Numerical calculations of the transverse intensity and phase profiles are shown in Fig. 4 in the regions (a) $x<0$ and (b) $x>0$, respectively, with $z/z_{\mathrm{NL}}\approx 16$ and $\Delta n_{\mathrm{NL}}/n_0=5\times 10^{-5}$. In a quasi-one-dimensional system, dark soliton stripes [10] are the stationary solutions of Eq. (1) [9], and they are evident in the numerical calculations shown in Fig. 4 [11] [along with some radiated (or nonsoliton) waves]. That is, if the needles were replaced with a long opaque strip (or wire) of constant width L, then $N\approx \pi L/w_{\mathrm{NL}}$ pairs of DSS's with soliton eigenvalues $\lambda_S=(1-\lambda_S^2)^{1/2}\cot(\lambda_S L/w_{\mathrm{NL}})$ would form. However, if the width changes slowly along the wire as $L(y)$, then fewer solitons are expected from the thinner regions, and none from regions where a gap exists. This is indeed what is observed in numerical calculations and experiments. What makes this tapered-wire case profoundly different and dynamically more complex than the straight-wire case is the occurrence of radiated waves that are not parallel to the soliton stripes. In Fig. 4 the tips of the needles are sources of such diffracted radiation. As in linear diffraction, those waves with higher transverse momentum $k_\perp$ propagate fastest in the plane. In Fig. 4, only those components with long periods remain in the shadow region of the tips, e.g., where black dots have appeared. The calculated phase profile [Fig. 4(b)] of these dots clearly shows that they are vortices. These results indicate that DSS's are generally robust to small-length-scale perturbations, but exhibit a convective instability when exposed to *long-period* transverse waves.

To achieve the same qualitative results in the laboratory, we used four needles in a cross configuration, with the tips separated by ≈ 10 μm. The additional set of needles were required to overcome the gross effect of self-defocusing, which tends to deflect the destabilizing wave vectors out of the beam center, i.e., away from the region where we expect vortices (this helps to explain why dark soliton stripes and grids are stable in experiments [10]). When the beam power exceeded ≈ 1.0 W, both the intensity and interferogram confirmed vortex formations, i.e., dark isolated spots would separate from the soliton stripes, and a line of constant phase would terminate at each spot. Figure 5 shows both dark soliton stripes and vortex nodes, as expected. The inset is an interferogram corresponding to the outlined vortex region; it confirms the existence of two vortices of opposite topological charge.

The onset of the instability can be understood, in part, by considering that the transverse soliton "velocity" [9] is given by $V_S=\lambda_S(\Delta n_{\mathrm{NL}}/n_0)^{1/2}$, where we will assume the soliton stripe is aligned along the x axis. When a transverse amplitude modulation is added to the field, e.g., $E\rightarrow E+\varepsilon\cos qx$, where $\varepsilon\ll E_\infty$, then the soliton velocity will also be modulated, i.e., $\Delta V_S/V_S=\Delta E/E_\infty+\Delta\lambda_S/\lambda_S$. (Similar modulations, though of finite extent and having a continuous distribution of wave vectors, occur when a diffracting source radiates transverse waves, as in Fig. 4.) This modulation may therefore sinusoidally distort a soliton stripe with the same period as the perturbation, $x_q=2\pi/q$ (at least initially), and may lead to soliton breakup and decay. This was suggested by Kuznetsov and Turitsyn, whose rigorous stability analysis predicts such an instability [12]. On the other hand, we find that this distortion can vanish (meaning the instability is convective) if the mean value of $\Delta V_S/V_S$ is zero when averaged over the characteristic propagation distance z_{NL}, i.e., when $z_q\equiv kx_q^2/\pi\ll z_{\mathrm{NL}}$ (or equivalently, $x_q\ll w_{\mathrm{NL}}$). These anticipated stable ($x_q\ll w_{\mathrm{NL}}$) and unstable ($x_q\gg w_{\mathrm{NL}}$) soliton regimes can in fact be seen in Fig. 4. While this soliton velocity argument predicts a stable regime, it cannot predict the development of vortices in the unstable regime; rather we must turn to hydrodynamic considerations.

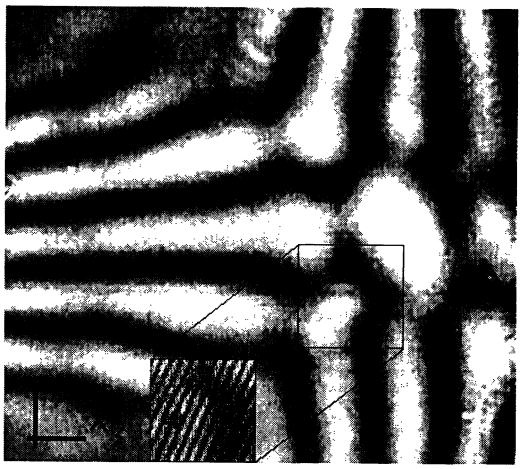

FIG. 5. Experimental observations of vortices spawned from dark soliton stripes. In the region corresponding to where the tips of four needles almost meet, dark nodes are seen, and the corresponding interferogram (inset) has the vortex signature (some lines have been darkened to aid the eye).

The occurrence of vortices and other fluid dynamic phenomena becomes evident once the NLS is rewritten in terms of the continuity equation, $\frac{1}{2}\partial\rho/\partial z+\nabla_\perp\cdot(\rho\mathbf{v})=0$, and the Bernoulli equations [Eq. (3)] for an inviscid compressible fluid. This transformation occurs upon setting $u=A\exp(i\phi)$ in Eq. (1) [7], and defining a phase velocity, or "flow," $\mathbf{v}=\nabla_\perp\phi$ (except at some singular points),

$$\partial\phi/\partial z+\mathbf{v}\cdot\mathbf{v}=\nabla_\perp^2\rho^{1/2}/\rho^{1/2}-P/\rho\,, \tag{3}$$

where $\rho=A^2$ and $P=\rho^2/2$ have the meanings of density and pressure, respectively. In this framework, the helical

phase profile in Eq. (2) is characterized by a "circulation" $\int_l \mathbf{v}\cdot d\boldsymbol{l} = \pm 2\pi$, where l is a closed path enclosing the vortex. The occurrence of vorticity in the field can be most easily shown by considering the explicit effects of a phase modulation (which occurs in quadrature with an amplitude modulation) added to the background field $\phi \rightarrow \phi[1+\varepsilon\sin(qx)]$, where $\varepsilon \ll 1$. When a DSS is aligned along the x axis, the phase on either side of the soliton is given by $\phi_S(y)[1+\varepsilon\sin(qx)]$, where $\phi_S(y)$ is the phase step associated with the soliton. The component of the phase velocity aligned along the soliton is then $\partial\phi/\partial x = \varepsilon q\phi_S(y)\cos(qx)$. A velocity *difference* therefore exists on either side of the soliton; hence the vorticity is nonzero. Periodic vorticity elements (but not yet vortices) will exist on the DSS at the positions $qx = N\pi$ (where N is an integer), with adjacent elements having opposite circulations. In fluids this phenomenon is known as a Kelvin-Helmholtz instability, which occurs when a boundary between two flow develops so-called vortex streets.

These considerations of the soliton velocity V_S and phase velocity $\nabla_\perp\phi$ indicate that a modulated DSS with $x_q \gg w_{\mathrm{NL}}$ will initially break into segments with counter-circulating vorticity at the ends. Bifurcation of the modulation period can result in further segmentation. The final collapse into vortices can be understood by considering that Eq. (3) is also the Hamilton-Jacobi equation [7], where the right-hand side is the potential term. The angular acceleration, $\partial^2\theta/\partial z^2 = \partial U/\partial\theta$ (where $U = A^2/2 - \nabla_\perp^2 A/A$), is therefore driven by the field and its Laplacian, and vanishes once Eq. (2) is satisfied, i.e., once the vortex is formed. Well-established hydrodynamic methods and paradigms may be applied to describe the dynamics of OVS's under more complex initial diffraction conditions. For example, using the vortex element technique [13], DSS's can be treated as two superposed vortex sheets having opposite charges per unit length. In summary, we have created single and paired optical vortex-soliton filaments in a self-defocusing optical Kerr medium. For an arbitrary initial condition, OVS's may develop if the average vorticity of the transverse phase velocity does not vanish over a distance z_{NL}.

This work was supported by the Defense Advanced Research Projects Agency, the Pittsburgh Supercomputing Center, and the Naval Research Laboratory (NRL). We especially thank E. M. Wright (University of Arizona) for suggesting that our observed nodes were vortices. We also thank D. W. Hess (NRL) for insights on superconductivity, E. A. Kuznetsov (Academy of Sciences, Novosibirsk) for instability discussions, and A. E. Kaplan (Johns Hopkins University) for comments on nonlinear propagation. G.A.S. is an Office of Naval Technology Postdoctoral Fellow.

[1] J. P. Gordon, R. C. C. Leite, R. S. Moore, S. P. S. Porto, and J. R. Whinnery, J. Appl. Phys. **36**, 3 (1965); A. G. Litvak, Pis'ma Zh. Eksp. Teor. Fiz. **4**, 341 (1966) [JETP Lett. **4**, 230 (1966)].

[2] V. L. Ginzburg and L. P. Pitaevskii, Zh. Eksp. Teor. Fiz. **34**, 1240 (1958) [Sov. Phys. JETP **7**, 858 (1958)]; L. P. Pitaevskii, Zh. Eksp. Teor. Fiz. **40**, 646 (1961) [Sov. Phys. JETP **13**, 451 (1961)].

[3] R. Y. Chiao, I. H. Deutsch, J. C. Garrison, and E. M. Wright, *Serge Akhmanov: A Memorial Volume,* edited by H. Walther (Adam Hilger, Bristol, 1992).

[4] J. F. Nye and M. V. Berry, Proc. R. Soc. London A **336**, 165 (1974); N. B. Baranova, A. V. Mamaev, N. F. Pilipetsky, V. V. Shkunov, and B. Ya. Zel'dovich, J. Opt. Soc. Am. **73**, 525 (1983).

[5] P. Coullet, L. Gil, and F. Rocca, Opt. Commun. **73**, 403 (1989); F. T. Arecchi, G. Giacomelli, P. L. Ramazza, and S. Residori, Phys. Rev. Lett. **67**, 3749 (1991); S. A. Akhmanov, M. A. Vorontsov, V. Yu. Ivanov, A. V. Larichev, and N. I. Zheleznykh, J. Opt. Soc. Am. B **9**, 78 (1992).

[6] R. Y. Chiao, E. Garmire, and C. H. Townes, Phys. Rev. Lett. **13**, 479 (1964); P. L. Kelley, Phys. Rev. Lett. **15**, 1005 (1965).

[7] W. G. Wagner, H. A. Haus, and J. H. Marburger, Phys. Rev. **175**, 256 (1968).

[8] See, for example, A. C. Newell, *Solitons in Mathematics and Physics* (Society for Industrial and Applied Mathematics, Philadelphia, 1985); E. Infeld and G. Rowlands, *Nonlinear Waves, Solitons and Chaos* (Cambridge Univ. Press, New York, 1990).

[9] V. E. Zakharov and A. B. Shabat, Zh. Eksp. Teor. Fiz. **64**, 1627 (1973) [Sov. Phys. JETP **37**, 823 (1973)].

[10] G. A. Swartzlander, Jr., D. R. Andersen, J. J. Regan, H. Yin, and A. E. Kaplan, Phys. Rev. Lett. **66**, 1583 (1991); **66**, 3321(E) (1991).

[11] These results where first reported in G. A. Swartzlander, Jr., in *Proceedings of III Potsdam-V Kiev International Workshop on Nonlinear Processes in Physics, August 1991* (Mathematics and Computer Science Department, Clarkson University, Potsdam, NY, 1991), and in G. A. Swartzlander, Jr., C. T. Law, D. R. Andersen, and A. E. Kaplan, in *Proceedings of the 1991 Annual Meeting of the Optical Society of America, November 1991,* Technical Digest Series Vol. 17 (Optical Society of America, Washington, DC, 1991).

[12] E. A. Kuznetsov and S. K. Turitsyn, Zh. Eksp. Teor. Fiz. **94**, 119 (1988) [Sov. Phys. JETP **67**, 1583 (1988)].

[13] See, for example, R. I. Lewis, *Vortex Element Methods for Fluid Dynamic Analysis of Engineering Systems* (Cambridge Univ. Press, New York, 1991).

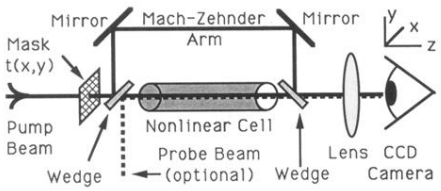

FIG. 1. Experimental apparatus. A laser beam passes through a mask with transmittance $t(x,y)$ near the input face of a nonlinear cell having $n_2 < 0$. The Mach-Zehnder interferometer allows phase measurements. A probe can be made to copropagate with the pump beam to observe wave guiding.

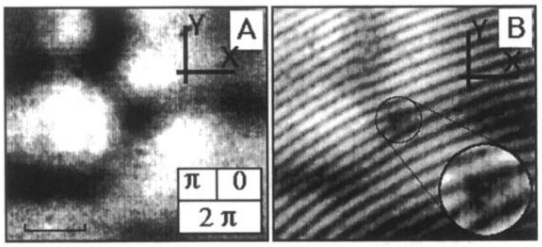

FIG. 2. Single-vortex-soliton experimental observations. (a) Intensity profile obtained with the phase mask shown in the inset. (b) Interferogram of (a), with magnified view of vortex region shown. The scale is 250 μm.

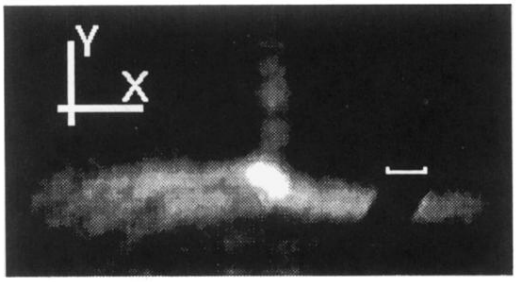

FIG. 3. Wave guiding of a He-Ne probe laser beam within an OVS filament. The phase mask in Fig. 2 was used, resulting in some leakage to dark soliton stripes. A wire of width 250 μm shows the relative size of the filament.

Figure 4

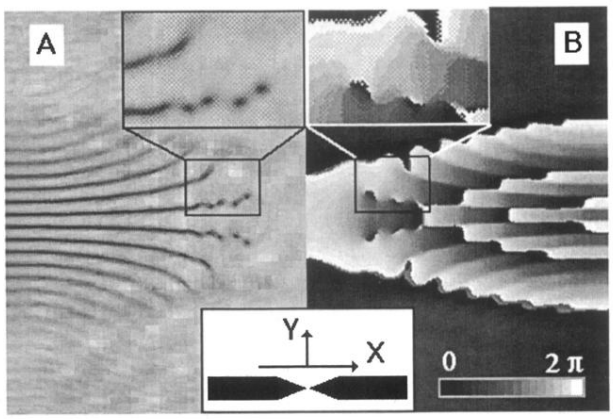

FIG. 4. Numerical calculations of intensity (a) and phase (b) profiles for nonlinear propagation past two needles, as shown in the bottom inset. Outside of the shadow region the solitons decay gracefully into the background. When subjected to long-period transverse perturbations, vortex pairs of opposite topological charge are formed owing to a Kelvin-Helmholtz instability.

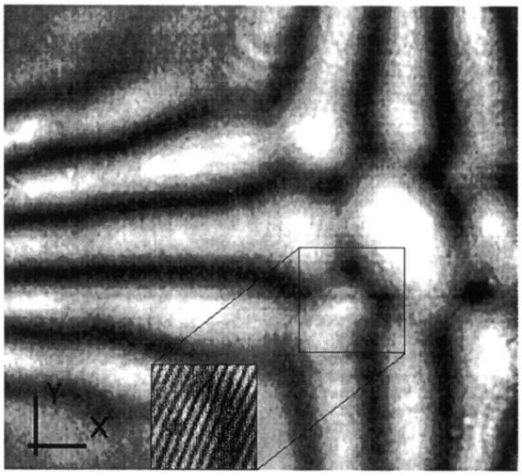

FIG. 5. Experimental observations of vortices spawned from dark soliton stripes. In the region corresponding to where the tips of four needles almost meet, dark nodes are seen, and the corresponding interferogram (inset) has the vortex signature (some lines have been darkened to aid the eye).